

1 **Geochemistry and isotopic composition ($\delta^{18}\text{O}$, $\delta^2\text{H}$, $^{87}\text{Sr}/^{86}\text{Sr}$, $^{143}\text{Nd}/^{144}\text{Nd}$) in**
2 **the groundwater of French Guiana as indicators of their origin and**
3 **interrelations**

4
5 **Géochimie et compositions isotopiques ($\delta^{18}\text{O}$, $\delta^2\text{H}$, $^{87}\text{Sr}/^{86}\text{Sr}$, $^{143}\text{Nd}/^{144}\text{Nd}$) des**
6 **eaux souterraines de Guyane comme indicateurs de leur origine et**
7 **interrelations**

8
9
10 **Philippe NÉGREL, Emmanuelle PETELET-GIRAUD**

11
12 B.R.G.M., Avenue C. Guillemin, BP 6009, 45060, Orléans Cedex 02, France,
13 e-mail: p.negrel@brgm.fr; e.petelet@brgm.fr

14
15
16 **Abstract** The current use of untreated river water for drinking purposes by the population of French Guiana has
17 important impacts on public health. Consequently, groundwater is of major importance as a possible alternative
18 drinking water supply to reduce these impacts. Since French Guiana belongs to the Guyana Shield, sustainable
19 water management can be expected to depend increasingly on water from fissured aquifers in hard rocks.
20 Groundwater samples were collected from shallow drill holes in the densely populated coastal area, and deeper
21 wells in the basement (around Cayenne and along the Maroni and Oyapock rivers). This study reports on major
22 and trace elements for which Na^+ and Ca^{2+} excess with regard to Cl reflect the role of water-rock interaction, as
23 well as Sr and Nd isotopes that reflect the role of the different lithologies. $\delta^{18}\text{O}$ and δD in waters give constraints
24 on the water cycle (recharge and evaporation processes).

25
26 **Résumé** L'utilisation d'eau de surface non traitée comme eau de boisson par la population guyanaise a des effets
27 importants en termes de santé publique. En conséquence, les ressources en eaux souterraines sont d'une
28 importance majeure comme alternative pour l'alimentation en eau potable afin de réduire les impacts sur la santé
29 publique. La Guyane française faisant partie du bouclier guyanais, les ressources en eau souterraine sont
30 probablement contenues dans les roches fracturées. Des eaux souterraines ont été prélevées dans des forages peu
31 profonds dans les zones de forte densité de population dans la zone côtière et dans des ouvrages plus profonds
32 dans les zones de socle (proche de Cayenne et le long des fleuves Maroni et Oyapock). Cette étude présente la
33 géochimie des éléments majeurs et traces pour lesquels les excès de Na^+ et Ca^{2+} par rapport au Cl reflètent le rôle
34 des interactions eau-roche tandis que les isotopes du Sr et Nd montrent le rôle des différentes lithologies
35 drainées. Les isotopes de la molécule d'eau ($\delta^{18}\text{O}$ et δD) tracent le cycle de l'eau, précisant la recharge et les
36 processus d'évaporation.

37
38 **Keywords:** French Guiana, Groundwater, Strontium isotopes, Neodymium isotopes

39
40 **Mots clés :** Guyane française, eau souterraine, isotopes du strontium, isotopes du néodyme

41

42 **1. Introduction**

43

44 Groundwater resources are of the utmost importance in French Guiana for water supply because the use of
45 untreated river water for drinking by the inland population induces important health impacts. Since French
46 Guiana belongs to the Guyana Shield, sustainable water management can be expected to depend increasingly on
47 water from fissured aquifers, e.g. mainly hard rocks (crystalline, metamorphic and volcanic rocks). The
48 exploitation of such fissured (heterogeneous and anisotropic) systems has to be linked to the characterisation of
49 aquifer structure and functioning, aquifer heterogeneities and relationships with surface water (Négrel and
50 Lachassagne, 2000; Négrel et al., 2002).

51 Present day research has to focus on increasing use of existing geochemical tools (such as Sr-Nd isotopes as well
52 as lead isotopes) dedicated to elucidate the structure and functioning of the different compartments of hard rock
53 aquifers, i.e. overlying sediments, when they do exist, weathered cover alterites, weathered-fissured zone,
54 fractured hard rock (Steinmann and Stille, 2006; Négrel, 2006). In particular, research will have to deal with the
55 identification of the relative signature of groundwater circulations in the alterites and in the underlying
56 weathered-fissured zone. This zone, with efficient porosities ranging from 3 to 20% in the alterites and from 0.5
57 to 2% in the weathered-fissured zone, may contain most of the groundwater reserve (since the efficient porosity
58 of fresh bedrock is often less than 0.01%). This will also help to identify the role of these different
59 hydrogeological compartments, both under natural and pumping conditions, and in the framework of surface-
60 groundwater relationships. These methods give better understanding of the alterites and underlying weathered-
61 fissured zone as hydrogeophysics, e.g. use of advanced geophysical methods to understand the interaction
62 between geology and fluid flow in the subsurface, did (Auken et al., 2009; Sailhac et al., 2009).

63 Since a sufficient number of boreholes have been drilled in French Guiana (Fig. 1), ongoing research is now
64 focusing on the geochemistry of ground waters for which the database will serve to build up a referential for this
65 region and will be valorised in conjunction with geologic, hydrodynamic, etc. data, as one main objective will be
66 to better define the functioning of French Guiana hard rock aquifers.

67

68 **2. General conditions in French Guiana**

69

70 French Guiana covers 10% of the Guyana Shield, which represents the northern extension of the Amazonian
71 Platform (Edmond et al., 1995; Deckart et al., 2005). The Guyana Shield comprises three rock complexes: the
72 Imataca Archaen gneiss (3.4-2.7 Ga), the Lower Proterozoic volcano-sedimentary terrains and granite-gneiss
73 rocks (2.3-1.9 Ga), and the Middle Proterozoic continental deposits and magmatic rocks (1.9-1.5 Ga). With
74 regard to its weathered substratum, which is composed only of Lower Proterozoic (2.5-1.9 Ga) igneous and
75 metamorphic rocks, French Guiana is similar to the Guyana Shield drained by the Orinoco (Edmond et al.,
76 1995). The geology of French Guiana can be summarized as four different units (Gruau et al., 1985; Deckart et
77 al., 2005) with the Cayenne Island series, the Lower Paramaca (hereafter referred to as unit P) of mainly
78 metavolcanic rocks and rare sediments, the Upper Paramaca (hereafter referred to as unit S) and Orapu
79 comprising schists, mica schists, quartzites, conglomerates, metagraywackes, metasiltites and rare metavolcanic
80 rocks and finally plutonic intrusions of gabbro-diorite, granite and granodiorite from the "Guyana plutonism",
81 and granitoid, granodiorite and tonalite from the "Caribbean plutonism".

82 The climatic and geodynamic conditions over the Guyana Shield since the Cretaceous have induced the
 83 extensive development of 50 to 100 m thick alterites masking the substratum (Driscoll and Karner, 1994). The
 84 climate is humid tropical, with two rainy seasons and two dry seasons and the total annual effective rainfall is
 85 around 1000 mm.y⁻¹. Most of the groundwater resource is located in the crystalline bedrock, typical of those of
 86 tropical hard rock settings. The alluvia have high clay content, mainly due to the nature of the sediments in
 87 tropical settings and also due to local weathering, they are relatively thin (mainly less than 5 m) and are of
 88 reduced lateral extent; they therefore account for only a small volume of groundwater. The alterites, which
 89 constitute the upper compartment of the bedrock aquifers, have an effective porosity of a few percent and thus a
 90 water storage function.

92 **3. Sampling procedures and analytical methods**

94 Groundwater samples (Fig.1) were collected 1) along the coastal area bordering the Atlantic Ocean from shallow
 95 drill holes in the extensive sandy-argillaceous terrane, mainly Holocene in age, (GWA/alt-sed in Table 1), which
 96 is the only densely populated area in French Guiana (Négre et al., 2002), 2) along the Maroni and Oyapock
 97 River catchments (Négre and Lachassagne, 2000) from shallow wells in the alluvia (GWA/alt-sed in Table 1).
 98 Groundwater samples were also collected from deep wells in the basement (Fig. 1), MM4, CAR1 and MKT2
 99 around Cayenne (GWA/bas in Table 1) from which groundwater is pumped from bedrock fractures, deep wells
 100 (GWA/bas in Table 1) in the basement along the two main rivers Maroni and Oyapock (F1, 2, M1, 3bis, 4, 5,
 101 L1bis, 2, CR1, 2) and more inland (Ni5).

102 Groundwater were filtered on site through 0.2 µm acetate cellulose filters and stored in pre-cleaned
 103 polypropylene bottles. The samples for cation and isotope measurements were acidified to pH 2 with ultrapure
 104 HNO₃, and one bottle of each sample (not acidified) was kept for anion determination. Electrical conductivity,
 105 water temperature and pH were measured in the field with a conductivity meter standardized to 20 °C and with a
 106 combined electrode and a pH-meter regularly calibrated using two standard buffers. Chemical analysis of the
 107 water samples was carried out by capillary ion electrophoresis for major cations and anions, by ICP-MS for Sr,
 108 Sm and Nd and HCl titration and Gran's method for the total alkalinity. Precision ranged between ± 5 and 10%
 109 for the determination of major and trace elements measurements. Classical methods for the separation by
 110 exchange column (cation for Sr, cation and HDEHP reverse chromatography for Nd) and isotope analysis
 111 (Finnigan MAT 262 multiple collector mass spectrometer) were used for Sr and Nd isotope measurements
 112 (Négre and Lachassagne, 1997; Négre et al., 2000). The reproducibility of ⁸⁷Sr/⁸⁶Sr measurement was tested by
 113 duplicate analyses of the NBS 987 standard (mean value 0.710227 ± 17.10⁻⁶, 2σ, n = 70) of the La Jolla
 114 international standard for Nd (¹⁴³Nd/¹⁴⁴Nd of 0.511826 ± 11.10⁻⁶, 2σ, n = 33). The ¹⁴³Nd/¹⁴⁴Nd ratios are
 115 expressed as εNd(0), which represents the deviation in parts per 10⁴ (ε unit) from ¹⁴³Nd/¹⁴⁴Nd in a chondritic
 116 reservoir with a present day CHUR value of 0.512636. Data are presented in Table 2.

117 **4. Results and Discussion**

120 **4.1. Chemical characterisation of waters**

121 The Total Dissolved Solids (TDS) fluctuates from 10 up to 166 mg.L⁻¹ in the groundwater from the extensive
 122 sandy-argillaceous terrane and from the alluvia (hereafter referred to as GWA/alt-sed) and from 46 to 218 mg.L⁻¹
 123

124 in the groundwater from the basement (hereafter referred to as GWA/bas). The water chemistry shows a large
 125 variation in major element contents (Table 2). Chloride content in the GWA/alt-sed groundwater ranges from 50
 126 to 4241 $\mu\text{mol.L}^{-1}$ and from 45 to 457 $\mu\text{mol.L}^{-1}$ in the GWA/bas groundwater. Though Cl^- ions do not have any
 127 significant lithological origin, since French Guiana is evaporite free, Cl^- ions in groundwater may originate
 128 mainly from rainfall recharge (sea salts, Gaillardet et al., 1997), and to a lesser extent from human activity
 129 (domestic sewage, fertilisers, etc). Chloride often behaves conservatively through the hydrological cycle and is
 130 used as an atmospheric-input reference element in many hydrosystems (Gaillardet et al., 1997). Like Cl^- , Na^+
 131 shows a wide range of contents and, when compared to Cl^- in Figure 2a, Na concentrations in most surface and
 132 ground waters plot above the seawater dilution line (SWDL), indicating Na^+ excess. Most of the surface and
 133 ground waters from the GWA/alt-sed plot between the SWDL and the line with a molar Cl/Na ratio of around
 134 0.5. Three GWA/bas ground waters (CR1, CR2 and F1-oct-98) plot with a molar Cl/Na ratio of 0.7, the
 135 hydrogeological data suggest that the alterite compartment contributes significantly to the well flow rate. The
 136 remaining GWA/bas ground waters plot with a molar Cl/Na ratio of 0.2. This divergence from the seawater
 137 dilution line reflects a large Na enrichment that is mainly related to water-rock interaction. Ca^{2+} concentrations
 138 show a large range in groundwater from about 5-10 to 999 $\mu\text{mol.L}^{-1}$ and fluctuate also largely in rain- and
 139 surface waters when compared to Cl^- in Figure 2b (all samples plot above the SWDL, with a Cl/Ca ratio of 1.42
 140 for the surface waters indicative of a Ca^{2+} excess). The groundwater from the GWA/alt-sed also display a Ca^{2+}
 141 excess and plot with a molar Cl/Ca ratio ranging between that of SWDL and the ratio 1.42, four of them plot
 142 with a molar Cl/Ca ratio higher than 1.42. The GWA/bas groundwater plot with a molar Cl/Ca ratio ranging
 143 between 1.42 and 0.05, reflecting the larger Ca^{2+} excess. Some of them plot with a molar Cl/Ca ratio of around
 144 1.42, close to the groundwater from the GWA/alt-sed, reflecting the fact that water partly originates from the
 145 alterite compartment. Similarly, K^+ , Mg^{2+} and Sr^{2+} excess are observed when plotted *versus* Cl^- , (not shown),
 146 reflecting the weathering of aluminosilicates.

147 The positive correlation between HCO_3^- and the sum of cations in groundwater samples (Σ^+ , $r^2 = 0.55$, $n = 38$)
 148 clearly indicates that the cations released by weathering are balanced by the alkalinity, in good agreement with
 149 observations in other South American basins influenced by similar climatic conditions (Gaillardet et al., 1997;
 150 Freyssinet and Farah, 2000). The bicarbonate increase during weathering originates from the atmospheric/soil
 151 CO_2 , which implies a positive correlation between HCO_3^- and pH in groundwater samples ($r^2 = 0.66$, $n = 38$)
 152 related to the water-rock interaction.

154 **4.2. Investigating groundwater recharge through $\delta^2\text{H}$ and $\delta^{18}\text{O}$ isotopic signature**

155
 156 Variations in the stable-isotope composition in a catchment's water balance are mainly caused by natural
 157 variations in the isotopic composition of rainfall and through mixing with pre-existing water and the influence of
 158 evaporation (Kendall and McDonnell, 1998). The stable isotopes $\delta^2\text{H}$ and $\delta^{18}\text{O}$ of all rain samples collected in
 159 French Guiana (Négrel et al., 1997) defines the local meteoric water line (LMWL), as illustrated in Figure 3a.
 160 The $\delta^{18}\text{O}$ and $\delta^2\text{H}$ in GWA/alt-sed ground waters fall in the range -2.1 to -3.7‰ for $\delta^{18}\text{O}$ and -7.9 to -19.2‰ for
 161 $\delta^2\text{H}$ and in the range -2.9 to -4.0‰ for $\delta^{18}\text{O}$ and -12.3 to -18.4‰ for $\delta^2\text{H}$ for the GWA/bas ground waters, in
 162 close agreement with the range of surface water (Négrel and Lachassagne 2000).

163 The $\delta^{18}\text{O}$ and $\delta^2\text{H}$ relationships are illustrated in Figure 3a and b for rainwater (regression line and 95%
 164 confidence range), global meteoric water line (GMWL; $\delta^2\text{H} = 8 \delta^{18}\text{O} + 10$, Craig, 1961), surface waters and
 165 groundwater. Surface waters plot close to the LMWL in Figure 3b and, as demonstrated by Négrel and
 166 Lachassagne (2000), most show a significant shift (close to 1.4‰) to the right of this line as result of evaporation
 167 processes. Most of the ground waters from GWA/alt-sed clearly plot close to the local and global lines. Some of
 168 these ground waters are displaced below the LMWL. This could be due either to evaporation prior or during
 169 infiltration or, as suggested by Boronina et al. (2005), because of partial evaporation from soils and dilution by
 170 subsequent recharge. GWA/bas groundwater also plot close to the LMWL and GMWL, reflecting a meteoric
 171 origin and a lack of significant evaporation during recharge or oxygen isotope exchanges between water and the
 172 rock matrix.

173 Infiltrating rainwater shows a mean weighted signatures for $\delta^{18}\text{O}$ and $\delta^2\text{H}$ of -4.51‰ and -24.23‰ respectively,
 174 corresponding to 1790.4 mm of rainfall (Négrel et al., 1997). However, mean rainwater δ -values cannot explain
 175 groundwater recharge as less negative values occur in many samples (Fig. 3b). Thus recharge from precipitation
 176 events occurs in significant amount at least during two periods. The first period was September to January and
 177 corresponds to the rainy season with 496 mm of rainfall (27.7% of the total annual rainfall, mean weighted rain
 178 signatures input led to $\delta^{18}\text{O}$ and $\delta^2\text{H}$ of around -2.45‰ and -7.58‰, respectively). The second period occurred in
 179 March-April with 249 mm rainfall, which corresponds to the middle of the rainy season (13.9% of the total
 180 annual rainfall, mean weighted rain input led to $\delta^{18}\text{O}$ and $\delta^2\text{H}$ signatures of around -3.10‰ and -11.11‰,
 181 respectively). These two rainy periods should constitute the recharge period that would explain the least negative
 182 δ -values in the ground waters. It is worth noting that part of the $\delta^{18}\text{O}$ and $\delta^2\text{H}$ signatures in the groundwater
 183 should reflect the recharge occurring during May to July. During this period, the rainfall was 943.3 mm, (52.7%
 184 of the total annual rainfall) and the mean weighted rain input led to $\delta^{18}\text{O}$ and $\delta^2\text{H}$ signatures of around -4.24‰
 185 and -20.89‰, respectively. This period of rain and thus recharge may explain the most negative δ -values in the
 186 groundwater samples. This suggests different stages of groundwater recharge with isotope signatures in close
 187 connection with the range in rainwater.
 188

189 **4.3. $^{87}\text{Sr}/^{86}\text{Sr}$ as a proxy of weathering processes**

190
 191 Sr isotope studies of rivers and lakes have shown that variations in $^{87}\text{Sr}/^{86}\text{Sr}$ and Sr contents are caused by
 192 mixing waters with different $^{87}\text{Sr}/^{86}\text{Sr}$ ratios and Sr contents, each of them reflecting water-rock interaction with
 193 different rock types (Oliver et al., 2003; Grove et al., 2003; Chung et al., 2009).

194 All the surface- and groundwater samples from French Guiana are plotted in a $^{87}\text{Sr}/^{86}\text{Sr}$ vs. $1/\text{Sr}$ diagram
 195 (Fig. 4a), which is classically used to evaluate two-component mixing and end-member water compositions.
 196 This figure indicates the existence of at least three end-members. The surface waters from the Maroni catchment,
 197 reported from Négrel and Lachassagne, 2000, plot along the mixing trend between the end-members
 198 corresponding to the drainage of the Unit P metavolcanic rocks (low $^{87}\text{Sr}/^{86}\text{Sr}$ ratio, highest [Sr]) and that of the
 199 Unit S meta-sedimentary lithology (highest $^{87}\text{Sr}/^{86}\text{Sr}$ ratio, intermediate [Sr]). The low $^{87}\text{Sr}/^{86}\text{Sr}$ ratio would
 200 reflect the weathering of rocks such as basalt and amphibolite that are known to impart a low $^{87}\text{Sr}/^{86}\text{Sr}$ ratio to
 201 the waters (Louvat and Allègre, 1997; Dessert et al., 2001) while the high $^{87}\text{Sr}/^{86}\text{Sr}$ ratio would be related to the
 202 weathering of schists and micaschists, which deliver higher $^{87}\text{Sr}/^{86}\text{Sr}$ ratios to the water (Aubert et al., 2002).

203 This compares to the results obtained on rivers draining “undifferentiated Proterozoic rocks” of the Guyana
204 Shield (Edmond et al., 1995), which also lie on the mixing trend between the S and P end-members. The third
205 end-member (intermediate $^{87}\text{Sr}/^{86}\text{Sr}$ ratio, low [Sr]) could correspond to the drainage of plutonic granitoid
206 intrusions ($\delta\eta$). In the Maroni catchment, the shift of some surface waters to the right of the mixing trend
207 between S and P end-members could reflect the input into the main stream of tributaries draining weathered
208 granitoids. This is also illustrated by some rivers from the GWA/alt-sed (Négrel et al., 2002) that plot in the field
209 $\delta\eta$ in the Figure 4a. Some ground waters from the same area plot very close to the mixing trend between S and P
210 end-members but most of them plot with a low $^{87}\text{Sr}/^{86}\text{Sr}$ ratio, reflecting the influence of the drainage of volcanic
211 rocks of the Lower Paramaca (Unit P). It is worth noting that some points of groundwater are shifted with a
212 higher 1/Sr ratio agreeing with the rainwater samples. Therefore it may be concluded that the shift reflects a
213 large rainwater input for the Sr budget compared to the Sr released by water-rock interaction.

214 The GWA/bas groundwaters lie on the straight line corresponding to a mixing between waters that have
215 interacted with rocks from Unit P and S. Most ground waters display the lowest $^{87}\text{Sr}/^{86}\text{Sr}$ ratio, reflecting the
216 interaction with rocks having a low Sr isotopic ratio. However, the location of the deep ground waters from
217 Grand Santi (F1, F2) is not consistent with an interaction with volcanic rocks of the Unit P because the boreholes
218 were drilled within granitoids. One way to explain the similarity between the drainage of volcanic rocks (Unit P)
219 and ground waters that have interacted with granitoids is to consider that the latter are influenced by the
220 weathering of low Rb-rich Sr phases, which would impart a low $^{87}\text{Sr}/^{86}\text{Sr}$ ratio to the waters. Weathering of low
221 Rb-rich Sr phases and more constraints on the $^{87}\text{Sr}/^{86}\text{Sr}$ ratio variations may be tested through a diagram
222 $^{87}\text{Sr}/^{86}\text{Sr}$ versus Ca/Na ratio (Fig. 4b). The use of a cation ratio rather than absolute concentrations alone, avoids
223 variations due to dilution or concentration effects (BenOthmann et al., 1997, Chung et al., 2009). As previously
224 detailed, when Ca is compared to Cl content (Fig. 2b), all ground waters are indicative of a Ca^{2+} excess, more
225 marked in the ground waters from the basement, as well as for Mg, while the Na enrichment is less. Thus, Ca/Na
226 appears to be a good indicator of weathering processes in waters from French Guiana. The surface water from
227 the Maroni catchment does not define a clear hyperbola that binary mixing should lead to (Langmuir et al.,
228 1978). They appear rather to be scattered along a main trend showing a large fluctuation in the $^{87}\text{Sr}/^{86}\text{Sr}$ ratio
229 with a weak Ca/Na range. This makes possible to define a first water-rock interaction process that corresponds to
230 surficial weathering of unit P and S. Surficial weathering of Unit S shows a larger $^{87}\text{Sr}/^{86}\text{Sr}$ ratio without changes
231 in the Ca/Na ratio. Rainwater field (RW in Fig. 4) shows a low Ca/Na ratio and a $^{87}\text{Sr}/^{86}\text{Sr}$ ratio around 0.710.
232 Two other trends can be defined with a weak fluctuation in the $^{87}\text{Sr}/^{86}\text{Sr}$ ratio within a change of the Ca/Na ratio.
233 The first trend corresponds to a water-rock interaction process from the surficial to the deep weathering of
234 granitoids. The deeper weathering of granitoids reflected in this trend implies that the weathering of Ca-bearing
235 phases (e.g. plagioclases and/or calcite, Pett-Ridge et al., 2009) is greater in sample MM4 than in sample CRM2.
236 The second trend corresponds to a water-rock interaction process from the surficial to the deep weathering of the
237 unit P with a weak fluctuation of the $^{87}\text{Sr}/^{86}\text{Sr}$ ratio (around 0.704) associated with a large increase in the Ca/Na
238 ratio. As for the first water-rock interaction processes, the shift towards a relatively high Ca/Na ratios can be
239 explained by more extensive weathering of Ca-bearing phases with a low $^{87}\text{Sr}/^{86}\text{Sr}$ ratio, such as plagioclase
240 and/or calcite. High Ca/Na ratios generally relate to carbonate weathering (Gaillardet et al., 1997), which is also
241 accompanied by increase in the Mg/Sr and Ca/Sr ratios (Rengarajan et al., 2009). The increase in the Ca/Na
242 ratios during the weathering of the unit P is accompanied by an increase of the Ca/Sr ratios (up to 500)

243 notwithstanding that this value is the lowermost value of carbonate weathering (Meybeck, 1986). On the other
 244 hand, large Ca/Na ratios were observed during basalt weathering (up to 3, Dessert et al.2001; Raiber et al., 2009;
 245 Rengarajan et al., 2009). Such large Ca/Na ratios were accompanied by Ca/Sr ratio around 500 (Dessert et
 246 al.2001). Thus we can conclude that the trend in the GWA/bas ground waters from the unit P may reflect a more
 247 intense weathering of Ca-bearing phases like plagioclases as no evidence of calcite has been reported in basalts.
 248 Using the $^{87}\text{Sr}/^{86}\text{Sr}$ and Ca/Na ratios of the extreme samples of the surficial and deep weathering of the unit P,
 249 which can be considered as end-members, a mixing line was calculated and reported in Figure 4b. The first end-
 250 member corresponds to the surficial weathering with a $^{87}\text{Sr}/^{86}\text{Sr}$ and Ca/Na ratios of around 0.703 and 0.4. The
 251 latter represents the value classically used for the weathering of silicate rocks (Gaillardet et al., 1997; Louvat and
 252 Allègre, 1997; Rengarajan et al., 2009). The second end-member shows a slightly higher $^{87}\text{Sr}/^{86}\text{Sr}$ ratio (i.e.
 253 0.705) and a greater Ca/Na ratio (i.e. 5). The calculation led to a divergence from the surficial weathering end-
 254 member of around 10% for F5, 25% for F2 and M4 and 50-60% for L1bis and L2.
 255

256 **4.4. Nd contents and Nd isotopes: implications for water–rock interactions**

257
 258 Since the development of the method by ICP-MS to determine the dissolved REE concentrations (Stetzenbach et
 259 al. 1994, Johannesson et al. 1995), many studies deal with the behaviour of the REE in continental waters
 260 (Gaillardet et al., 1997; Viers et al., 2000; Andersson et al., 2001; Janssen and Verweij, 2003 and references
 261 therein) but, in contrast, neodymium isotopes have not been extensively used in hydrogeological studies. Some
 262 data are available on the compositions of river water (Goldstein and Jacobsen, 1987; Tricca et al., 1999;
 263 Andersson et al., 2001; Steinmann and Stille, 2006) and very little information is available for saline waters
 264 (Négrel 2006) and ground waters (Tricca et al., 1999; Viers and Wasserburg, 2004). The contents of Sm and Nd,
 265 as well as for the other dissolved REEs vary greatly. The dissolved Nd content in the surface waters varies from
 266 20 to 102 ng.L^{-1} with a low TDS (10-20 mg.L^{-1}), in agreement with values reported by other studies (Amazon,
 267 Gaillardet et al., 1997; Cameroon, Viers et al., 2000, Viers and Wasserburg, 2004) but broadly independent of
 268 other parameters such as total dissolved solids and pH. In the groundwater from the GWA/alt-sed, the dissolved
 269 Nd content varies from 39 to 752 ng.L^{-1} together with a broad range in the TDS (10 up to 166 mg.L^{-1}). In the
 270 GWA/bas groundwater, the dissolved Nd contents are lower and vary from 3 to 63 ng.L^{-1} with TDS values
 271 ranging from 46 to 218 mg.L^{-1} . These ranges agree with other studies in groundwater (Oliva et al., 1999; Viers
 272 and Wasserburg, 2004). As usually stated in terrestrial surface processes and in granite-gneiss rocks, Sm displays
 273 similar behaviour to Nd ($\text{Nd} = 4.9 \times \text{Sm} + 6.5$, $r^2 = 0.98$, $n = 30$), because of the similarity in their physical and
 274 chemical properties (Goldstein and Jacobsen, 1987; Gaillardet et al., 1997; Viers and Wasserburg, 2004). The
 275 isotopic composition of dissolved Nd in surface and ground waters from French Guiana ranges from $^{143}\text{Nd}/^{144}\text{Nd}$
 276 $= 0.511377 \pm 9.10^{-6}$ to 0.512162 ± 8.10^{-6} corresponding to a range of $\epsilon\text{Nd}(0)$ from -9.2 to -24.6. The lowest
 277 $\epsilon\text{Nd}(0)$ are observed in the GWA/alt-sed groundwater whereas the highest are for the GWA/bas groundwater.
 278 The small differences between $\epsilon\text{Nd}(0)$ values for both the dissolved and suspended phases found within the same
 279 rivers suggests that the Nd isotopic composition can be used as an indicator of the weathered parent rock
 280 (Goldstein and Jacobsen, 1987, 1988; Tricca et al., 1999). Mixing processes and water–rock interaction have
 281 both contributed to the observed $\epsilon\text{Nd}(0)$ (Négrel et al., 2001).

282 The similarity between the $^{143}\text{Nd}/^{144}\text{Nd}$ ratios in waters and related bedrock can be postulated now according to
 283 the recent works by Aubert et al. (2001). Comparing the Nd and Sr isotopic composition in minerals and waters,
 284 they demonstrated that the Sr and Nd isotopic characteristics of the major mineral phases of a granite clearly
 285 shows the strong influence of plagioclase and phosphate minerals (e.g. apatite) on the isotopic composition of
 286 the spring and stream waters. This was confirmed on other granite massif (France) by Négrel (2006). Thus,
 287 comparison of the $\epsilon\text{Nd}(0)$ values with the corresponding Sm/Nd ratios (e.g. $^{147}\text{Sm}/^{144}\text{Nd}$ ratios represented with
 288 the propagate errors) yields more information about the origin of the REE in the waters from French Guiana
 289 (Fig. 5). With the exception of the samples GUY99-11 and F1, they are positively correlated ($\epsilon\text{Nd}(0) = -43.3 +$
 290 $233.8 \times ^{147}\text{Sm}/^{144}\text{Nd}$; $r^2 = 0.64$; $n = 16$) with low $^{147}\text{Sm}/^{144}\text{Nd}$ ratios for the river water and rather high ratios for
 291 the ground waters.

292 Most of the ground waters have $^{147}\text{Sm}/^{144}\text{Nd}$ ratios significantly higher than the average continental crust value
 293 of 0.105 (Allègre and Lewin, 1989). The $\epsilon\text{Nd}(0)$ vs. the $^{147}\text{Sm}/^{144}\text{Nd}$ ratio in the surface water and GWA/bas
 294 groundwater, illustrated in Figure 5, are consistent with that of the parent rocks (Gruau et al., 1985; Delor et al.,
 295 2001). If the $\epsilon\text{Nd}(0)$ is mostly controlled by the weathering of plagioclase and phosphate phases, as suggested by
 296 Aubert et al. (2001) and Négrel (2006), they should be shifted towards higher $\epsilon\text{Nd}(0)$ and Sm/Nd ratios and thus
 297 would plot on the right of the parent rocks field, which is not observed. The $\epsilon\text{Nd}(0)$ vs. the $^{147}\text{Sm}/^{144}\text{Nd}$ ratio for
 298 the groundwater from the GWA/alt-sed plot between the values measured in the parent rocks and that of
 299 suspended matter from the Amazon Basin (Goldstein et al., 1984; Allègre et al., 1996). This suggests for some
 300 groundwater a possible influence of sedimentary deposits in the coastal area that originate from the Amazon. The
 301 other groundwater from the same area agree with the field of parent rocks, suggesting that Nd originates from the
 302 weathering of the bedrock.

304 5. Summary and perspectives

306 We report the dissolved concentrations of major and trace elements, stable isotopes (O and D), strontium
 307 ($^{87}\text{Sr}/^{86}\text{Sr}$) and neodymium isotopes ($^{143}\text{Nd}/^{144}\text{Nd}$) in ground waters and surface waters in French Guiana.
 308 Groundwater samples were collected from (i) shallow drill holes in this coastal area, which is the only densely
 309 populated area in French Guiana, and (ii) deeper wells in the basement from which groundwater is pumped from
 310 bedrock fractures.

311 Major cations show excess due to water-rock interaction. Comparing $\delta^{18}\text{O}$ and $\delta^2\text{H}$ reveals that most ground
 312 waters agree with both local and global meteoric water lines without evaporation impacts. The $^{87}\text{Sr}/^{86}\text{Sr}$ ratios
 313 indicate the existence of at least three end-members that corresponds respectively to the drainage of
 314 metavolcanic rocks, meta-sedimentary lithology and plutonic granitoid intrusions. The $^{87}\text{Sr}/^{86}\text{Sr}$ and Ca/Na ratios
 315 yield evidence of increase in the weathering of metavolcanic rocks with the larger divergence between surficial
 316 and deep weathering of about 60%. The $\epsilon\text{Nd}(0)$ in some ground waters reveals a possible influence of
 317 sedimentary deposits in the coastal area that originate from the Amazon and on the other hand, some ground
 318 waters plot in agreement with the field of parent rocks, suggesting that Nd originates from the weathering of the
 319 bedrock. This geochemical and isotopic approach to the groundwater in French Guiana has allowed the origin
 320 and complex relationships between the different compartments of the hard-rock aquifers to be more clearly
 321 defined.

322

323 **Acknowledgements** This work was funded by the BRGM Research Division. Chemical and isotopic analyses
324 were performed in the Geochemistry Laboratory of the BRGM, France. We thank the two anonymous reviewers
325 for providing critical comments that improved this manuscript. We are grateful to Dr. H.M. Kluijver for
326 proofreading and editing the English text.

327

328 **References**

329

330 Allègre CJ, Lewin, E (1989) Chemical structure and history of the Earth: evidence from global non-linear
331 inversion of isotopic data in a three-box-model. *Earth and Planetary Science Letters* Vol 96: 61-88.

332 Allègre CJ, Dupré B, Négrel Ph, Gaillardet J (1996) Sr-Nd-Pb isotopes systematics in Amazon and Congo River
333 systems. *Constraints about erosion processes. Chemical Geology* Vol 131: 93-112.

334 Andersson PS, Dahlgvist R, Ingri J, Gustafsson Ö (2001) The isotopic composition of Nd in a boreal river: A
335 reflection of selective weathering and colloidal transport. *Geochimica Cosmochimica Acta* Vol 65: 521–
336 527.

337 Aubert D, Stille P, Probst A (2001) REE fractionation during granite weathering and removal by waters and
338 suspended loads: Sr and Nd isotopic evidence. *Geochimica Cosmochimica Acta* Vol 65: 387-406.

339 Aubert D, Probst A, Stille P, Viville D (2002) Evidence of hydrological control of Sr behavior in stream water
340 (Strengbach catchment, Vosges mountains, France). *Applied Geochemistry* Vol 17: 285-300.

341 Auken E, Violette S, d'Ozouville N, Deffontaines B, Sorensen K, Viezzoli A, de Marsily G (2009) An
342 integrated study of the hydrogeology of volcanic islands using airborne transient electromagnetic:
343 Application in the Galapagos Archipelago, C. R. *Geoscience* vol 341: 899–907.

344 BenOthmann D, Luck JM, Tournoud MG (1997) Geochemistry and water dynamics: application to short time-
345 scale flood phenomena in a small Mediterranean catchment. I. Alkalis, alkali-earth and Sr isotopes.
346 *Chemical Geology* Vol 140: 9-28.

347 Boronina A, Balderer W, Renard P, Stichler W (2005) Study of stable isotopes in the Kouris catchment (Cyprus)
348 for the description of the regional groundwater flow. *Journal of Hydrology* Vol 308: 214-226.

349 Chung CH, You CF, Chu HY (2009) Weathering sources in the Gaoping (Kaoping) river catchments,
350 southwestern Taiwan: Insights from major elements, Sr isotopes, and rare earth elements. *Journal of*
351 *Marine Systems* Vol 76: 433-443.

352 Craig H 1961. Isotopic variations in meteoric water. *Science*, 133, 1702-1703.

353 Delor C, Egal E, Lahondere D, Marteau P (2001) Carte géologique de la Guyane, 1/500000, 2ed, BRGM eds.

354 Deckart K, Bertrand H, Liégeois JP (2005) Geochemistry and Sr, Nd, Pb isotopic composition of the Central
355 Atlantic Magmatic Province (CAMP) in Guyana and Guinea. *Lithos* Vol 82 : 289-314.

356 Dessert C, Dupré B, François LM, Schott J, Gaillardet J, Chakrapani G, Bajpai S (2001) Erosion of Deccan
357 Traps determined by river geochemistry: impact on the global climate and the $^{87}\text{Sr}/^{86}\text{Sr}$ ratio of seawater.
358 *Earth and Planetary Science Letters* Vol 188: 459-474.

359 Driscoll NW, Karner GD (1994) Flexural deformation due to Amazon fan loading: a feedback mechanism
360 affecting sediment delivery to margins. *Geology* Vol 22: 1015-1018.

361 Edmond JM, Palmer MR, Measures CI, Grant B, Stallard RF (1995) The fluvial geochemistry and denudation
362 rate of the Guayana shield in Venezuela. *Geochimica Cosmochimica Acta* Vol 59, 16: 3301-3325.

363 Freyssinet P, Farah AS (2000) Geochemical mass balance and weathering rates of ultramafic schists in
364 Amazonia. *Chemical Geology* Vol 170: 133-151.

365 Gaillardet J, Dupré B, Allègre CJ, Négrel Ph (1997) Chemical and physical denudation in the Amazon river
366 basin. *Chemical Geology* Vol 142:141-173.

367 Goldstein SJ, Jacobsen SB (1987) The Nd and Sr Isotopic systematics of river-water dissolved material:
368 implications for the sources of Nd and Sr in seawater. *Chemical Geology* Vol 66: 245-272.

- 369 Goldstein SJ, Jacobsen SB (1988) Nd and Sr isotopic systematics of river water suspended material: implications
370 for crustal evolution. *Earth and Planetary Science Letters* Vol 87: 249–265.
- 371 Goldstein SL, O’Nions RK, Hamilton PJ (1984) A Sm-Nd isotopic study of atmospheric dusts and particulates
372 from major river systems *Earth and Planetary Science Letters* Vol 70: 221–236.
- 373 Grove MJ, Baker PA, Cross SL, Rigsby CA, Seltzer GO (2003) Application of strontium isotopes to
374 understanding the hydrology and paleohydrology of the Altiplano, Bolivia–Peru. *Palaeogeography*
375 *Palaeoclimatology Palaeoecology* Vol 194: 281–297.
- 376 Gruau G, Martin H, Leveque B, Capdevilla R, Marot A (1985) Rb-Sr and Sm-Nd geochronology of lower
377 Proterozoic granite-greenstone terrains in French Guiana, South America. *Precambrian Research* Vol 30:
378 63–80.
- 379 Janssen RPT, Verweij W (2003) Geochemistry of some rare earth elements in groundwater, Vierlingsbeek, The
380 Netherlands. *Water Research* Vol 37: 1320–1350.
- 381 Johannesson KH, Lyons WB (1995) Rare earth element geochemistry of Colour Lake, an acidic freshwater lake
382 on Axel Heiberg Island, Northwest Territories, Canada. *Chemical Geology* vol 119: 209–223.
- 383 Kendall C, McDonnell JJ (1998) *Isotope Tracers in Catchment Hydrology*. Elsevier, 839 p.
- 384 Langmuir CH, Vocke RD, Hanson GN, Hart SR (1978) A general mixing equation with application to Icelandic
385 basalts. *Earth and Planetary Science Letters* Vol 37: 380–392.
- 386 Louvat P, Allègre CJ (1997) Present denudation rates on the island of Reunion determined by river
387 geochemistry: basalt weathering and mass budget between chemical and mechanical erosions.
388 *Geochimica Cosmochimica Acta* Vol 61: 3645–3669.
- 389 Meybeck, M (1986) Composition chimique des ruisseaux non pollués de France. *Sciences Geologiques Bulletin*
390 Vol 39 : 3–77.
- 391 Nègre Ph, Lachassagne P, Laporte P (1997) Caractérisation chimique et isotopique des pluies de Cayenne
392 (Guyane Française). *C.R. Académie des Sciences* 324: 379–386.
- 393 Nègre Ph, Lachassagne P (2000) Geochemistry of the Maroni River (French Guyana) during low water stage:
394 Implications for water rock interaction and groundwater characteristics. *Journal of Hydrology* Vol 237:
395 212–233.
- 396 Nègre Ph, Petelet-Giraud E, Casanova J, Kloppmann W (2002) Boron isotope signatures in the coastal
397 groundwaters of French Guiana. *Water Resources Research*. <http://www.agu.org/> DOI:
398 10.1029/2002WR001299 Art. No. 1262 cited Nov 2002.
- 399 Nègre Ph (2006) Water-granite interaction: clues from strontium, neodymium and rare earth elements in
400 saprolite, sediments, soils, surface and mineralized waters. *Applied Geochemistry* Vol 21: 1432–1454.
- 401 Oliver L, Harris N, Bickle M, Chapman H, Dise N, Horstwood M (2003) Silicate weathering rates decoupled
402 from the $^{87}\text{Sr}/^{86}\text{Sr}$ ratio of the dissolved load during Himalayan erosion. *Chemical Geology* Vol 201: 119–
403 139.
- 404 Oliva P, Viers J, Dupré B, Fortuné JP, Martin F, Braun JJ, Nahon D, Robain H (1999) The effect of organic
405 matter on chemical weathering: study of a small tropical watershed: Nsimi-Zoétéélé site, Cameroon.
406 *Geochimica Cosmochimica Acta* Vol 63: 4013–4035.
- 407 Pett-Ridge JC, Derry LA, Kurtz AC (2009) Sr isotopes as a tracer of weathering processes and dust inputs in a
408 tropical granitoid watershed, Luquillo Mountains, Puerto Rico. *Geochimica et Cosmochimica Acta* Vol
409 73: 25–43.
- 410 Raiber M, Webb JA, Bennetts DA (2009) Strontium isotopes as tracers to delineate aquifer interactions and the
411 influence of rainfall in the basalt plains of southeastern Australia. *Journal of Hydrology* Vol 367: 188–
412 199.
- 413 Rengarajan R, Singh SK, Sarin MM, Krishnaswami S (2009) Strontium isotopes and major ion chemistry in the
414 Chambal River system, India: Implications to silicate erosion rates of the Ganga. *Chemical Geology* Vol
415 260: 87–101.
- 416 Sailhac P, Bano M, Behaegel M, Girard J-F, Falgàs Para E, Ledo J, Marquis G, Matthey P-D, Ortega-Ramírez J
417 (2009) Characterizing the vadose zone and a perched aquifer near the Vosges ridge at the La Soutte
418 experimental site, Obernai, France, *C. R. Geoscience* vol 341: 818–830.

- 419 Steinmann M, Stille P (2006) Rare earth element transport and fractionation in small streams of a mixed
420 basaltic–granitic catchment basin (Massif Central, France). *Journal of Geochemical Exploration* Vol 88:
421 336-340.
- 422 Stetzenbach K J, Amano M, Kreamer D K, Hodge V F (1994) Testing the limits of ICP-MS: Determination of
423 trace elements in groundwater at the pert-per-trillion level. *Groundwater* Vol 32: 976-985.
- 424 Tricca A, Stille P, Steinman M, Kiefel B, Samuel J, Eikenberg J (1999) Rare earth elements and Sr and Nd
425 isotopic compositions of dissolved and suspended loads from small river systems in the Vosges
426 mountains (France), the river Rhine and groundwater. *Chemical Geology* Vol 160: 139–158.
- 427 Viers J, Dupré, B, Braun JJ, Deberdt S, Angeletti B, Ngoupayou JN, Michard A (2000) Major and trace element
428 abundances, and strontium isotopes in the Nyong basin rivers (Cameroon): constraints on chemical
429 weathering processes and elements transport mechanisms in humid tropical environments. *Chemical*
430 *Geology* Vol 169: 211-241.
- 431 Viers J, Wasserburg GJ (2004) Behavior of Sm and Nd in a lateritic soil profile. *Geochimica Cosmochimica*
432 *Acta* Vol 68: 2043-2054.
433

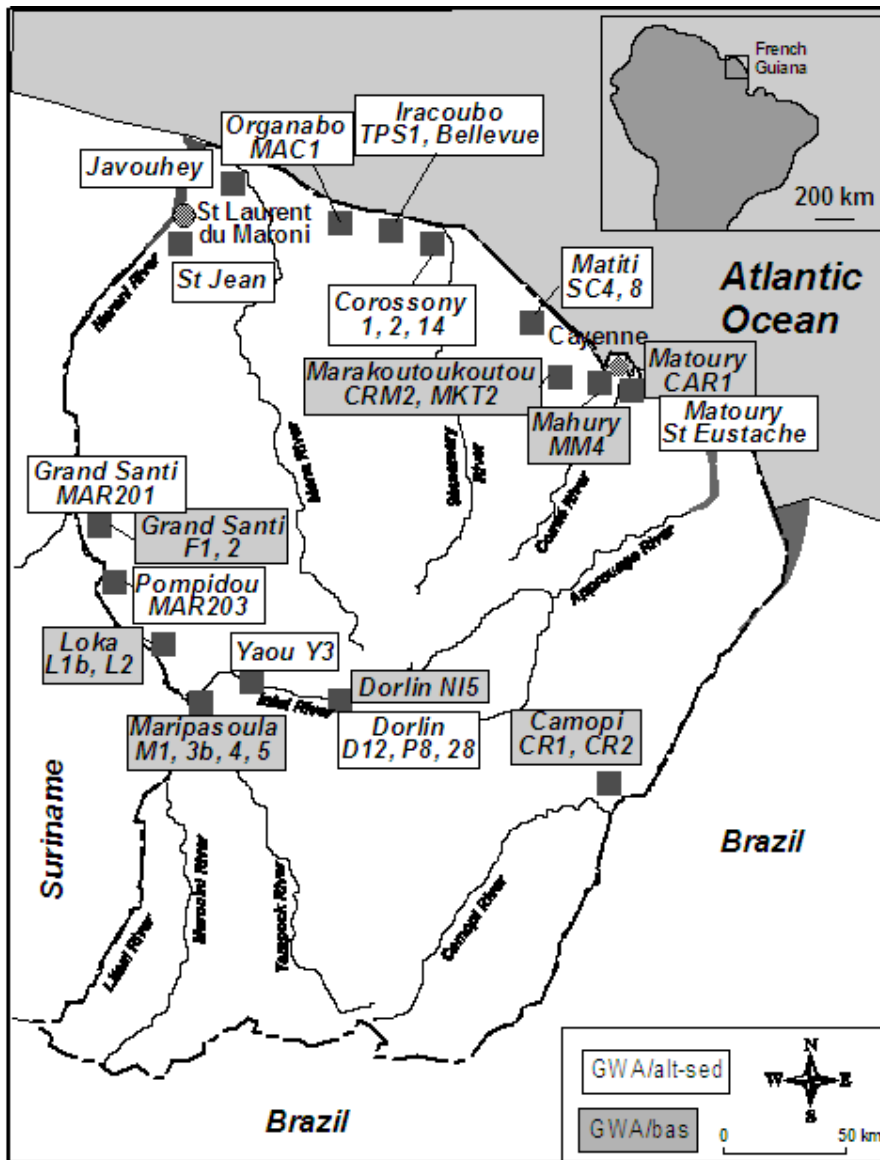
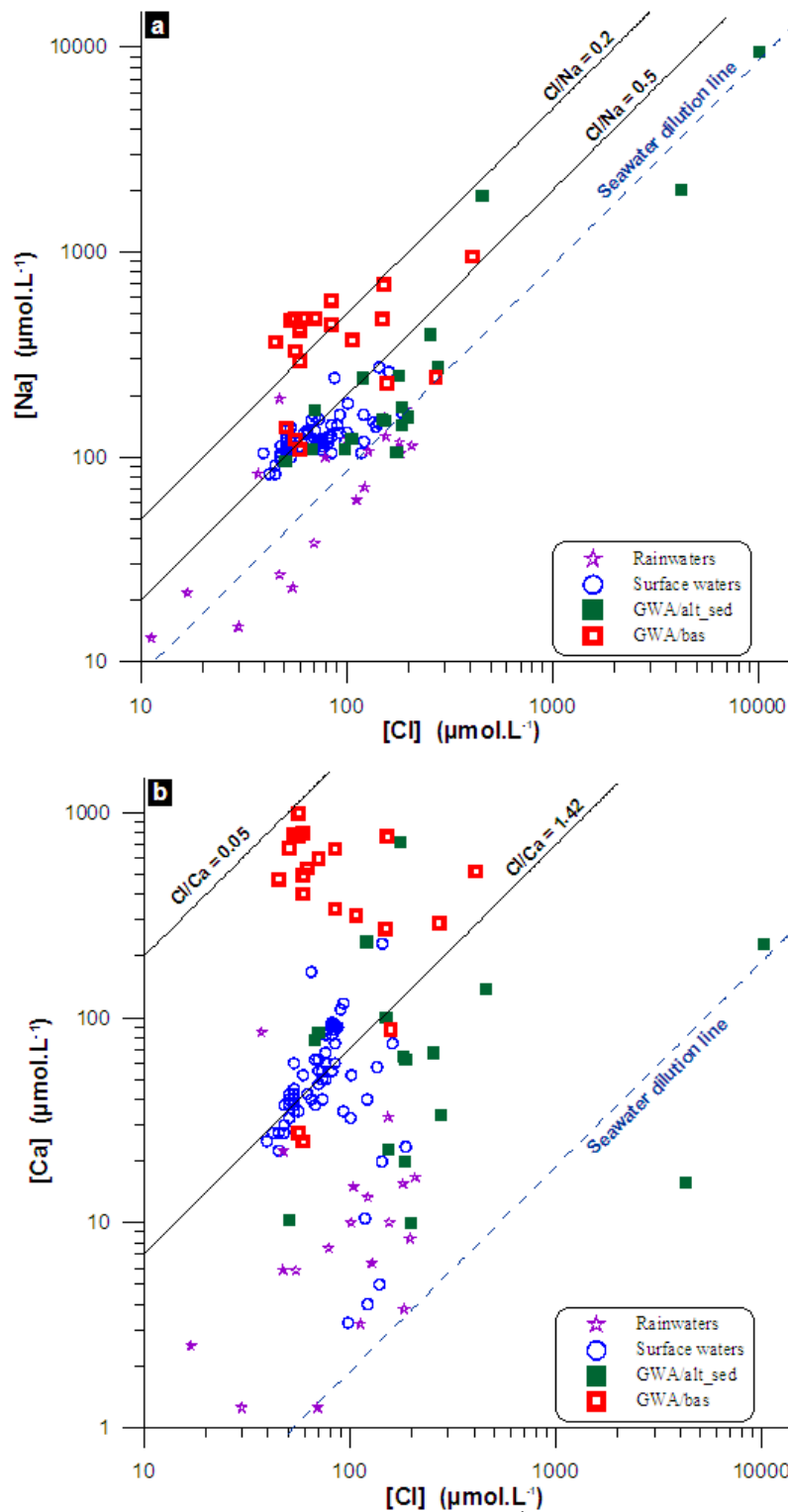


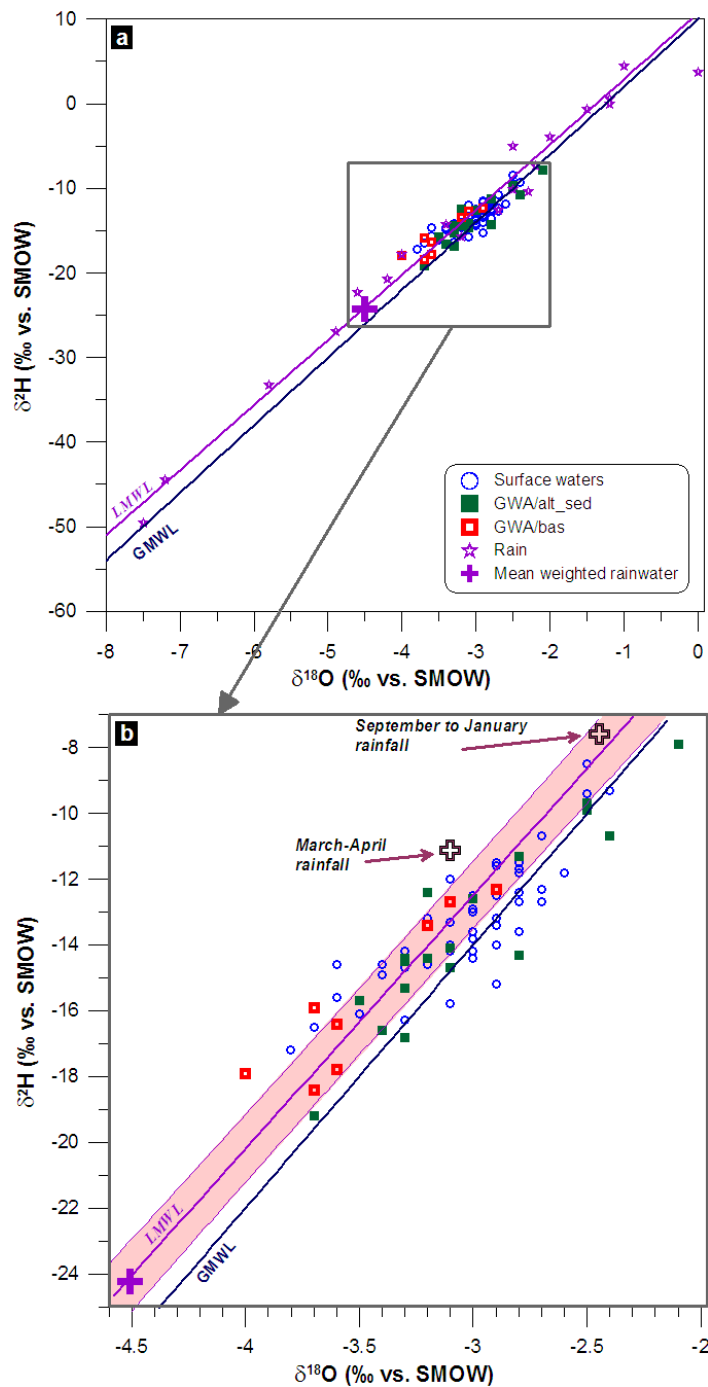
Figure 1. Map showing the site locations in French Guiana where groundwaters were sampled and analysed for major ions and isotope systematics.

Figure 1. Carte de localisation des sites d'échantillonnage des eaux souterraines en Guyane pour analyses des ions majeurs et des isotopes.



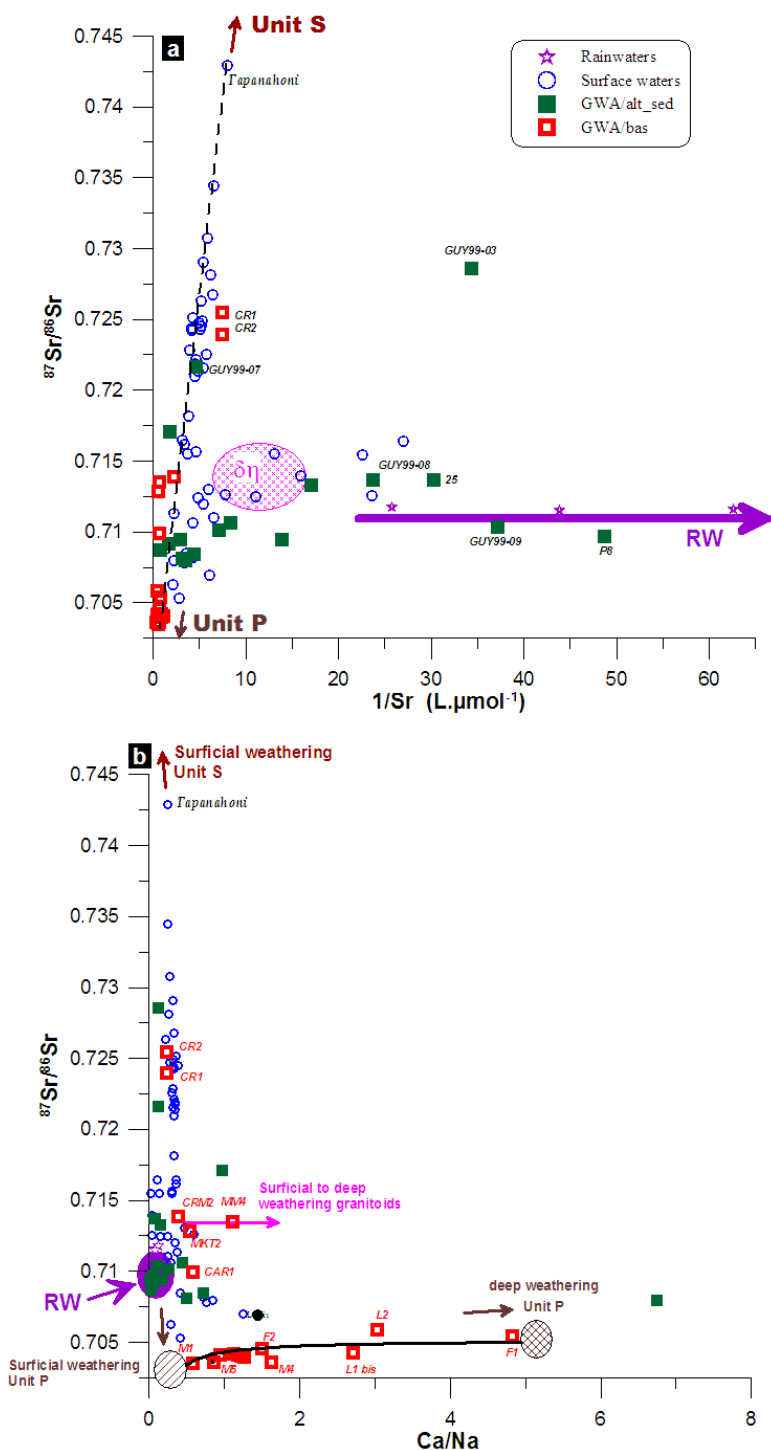
442
443 Figure 2. a) Cl vs. Na concentrations (in $\mu\text{mol.l}^{-1}$) in surface- and groundwaters from French Guiana. b) vs. Ca
444 Ca concentrations (in $\mu\text{mol.l}^{-1}$) in surface- and groundwaters from French Guiana. Rainwater data are from Négrel
445 et al. (1997) and surface water data are from Négrel and Lachassagne (2000).
446

447 *Figure 2. a) Concentrations des eaux de surface et souterraines de Guyane en Cl et Na (en $\mu\text{mol.l}^{-1}$). b) Cl vs.*
448 *Ca (en $\mu\text{mol.l}^{-1}$) dans les eaux de surface et souterraines de Guyane. Les données des eaux de pluies sont*
449 *extraites de Négrel et al. (1997); celles des eaux de surface sont extraites de Négrel et Lachassagne (2000).*

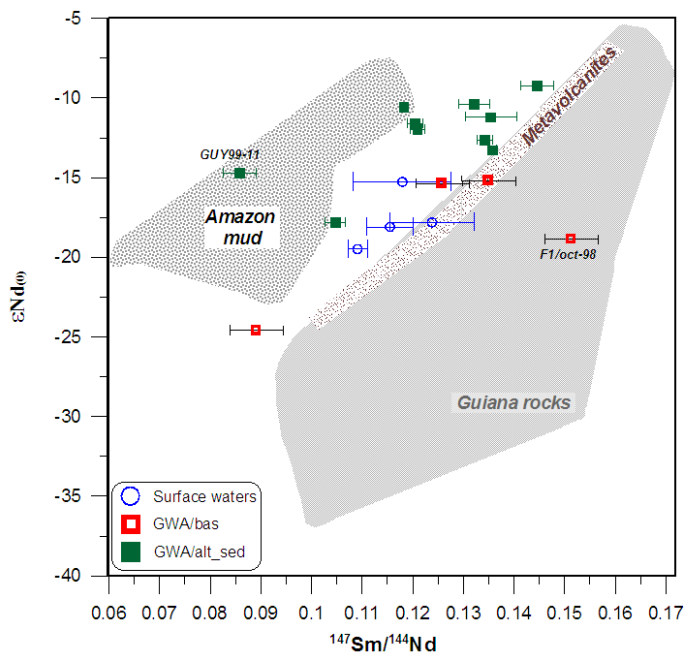


450
 451 Figure 3. Relationships between $\delta^2\text{H}$ and $\delta^{18}\text{O}$ (‰ vs. SMOW Standard Mean Ocean Water) in surface- and
 452 groundwaters collected from French Guiana (a). Rainwater data, e.g. Local Meteoric Water Line LMWL, i.e. 10
 453 monthly accumulations and 3 individual rain events in Cayenne (Négrel et al., 1997) and 6 rain events in the
 454 Maroni catchment (Négrel and Lachassagne 2000) are shown together with the Global Meteoric Water Line
 455 (GMWL: Craig, 1961); see text for origin of additional data. The big cross indicates the mean weighted rain
 456 input. In the extended view (b), the regression line and error bar envelope are indicated for the LMWL.
 457

458 *Figure 3. Relations entre $\delta^2\text{H}$ et $\delta^{18}\text{O}$ (‰ vs. SMOW Standard Mean Ocean Water) dans les eaux de surface et*
 459 *souterraines de Guyane (a). Les données des pluies, e.g. droite météorique locale (LMWL, i.e. 10 échantillons*
 460 *mensuels intégrés, 3 pluies individuelles à Cayenne (Négrel et al., 1997) et 6 pluies individuelles dans le bassin*
 461 *versant du Maroni (Négrel and Lachassagne 2000) sont illustrées avec la droite météorique mondiale (Global*
 462 *Meteoric Water Line GMWL: Craig, 1961). Les croix sur le schéma indiquent les valeurs moyennes pondérées*
 463 *des pluies. Dans la vue étendue (b), sont indiquées la droite de régression et les enveloppes d'incertitudes pour*
 464 *la roite météorique locale LMWL.*



465
 466 Figure 4. Relationship between a) $^{87}\text{Sr}/^{86}\text{Sr}$ ratios and $1/\text{Sr}$ and b) $^{87}\text{Sr}/^{86}\text{Sr}$ ratios and Ca/Na ratios in surface-
 467 and groundwaters collected from French Guiana. Rainwater data are from Négrel et al. (1997) and surface water
 468 data are from Négrel and Lachassagne (2000). **Unit S**: schistes, micaschistes, quartzites, conglomérats,
 469 métagrauwackes, métasiltites. **Unit P**: roches méta-volcaniques (basalte, amphibolite) et rare
 470 sédiments. $\delta\eta$: intrusions gabbro-dioritiques, granite et granodiorite.
 471
 472 *Figure 4. Relation entre a) rapports $^{87}\text{Sr}/^{86}\text{Sr}$ et $1/\text{Sr}$ et b) rapports $^{87}\text{Sr}/^{86}\text{Sr}$ et rapports Ca/Na dans les eaux de
 473 surface et souterraines de Guyane. Les données des eaux de pluies sont extraites de Négrel et al. (1997); celles
 474 des eaux de surface sont extraites de Négrel et Lachassagne (2000). **Unit S**: schistes, micaschistes, quartzites,
 475 conglomérats, métagrauwackes, métasiltites. **Unit P**: roches méta-volcaniques (basalte, amphibolite) et rare
 476 sédiments. $\delta\eta$: intrusions gabbro-dioritiques, granite et granodiorite.*



477
478 Figure 5. Plot of $\epsilon Nd(0)$ vs. $^{147}Sm/^{144}Nd$ in surface- and groundwaters collected from French Guiana. Bedrock
479 whole rocks $\epsilon Nd(0)$ fields are from Gruau et al. (1985); Delor et al. (2001) and Deckart et al. (2005) and the
480 Amazon suspended matter data are from Allègre et al. (1996).
481

482 *Figure 5. Diagramme entre $\epsilon Nd(0)$ vs. $^{147}Sm/^{144}Nd$ dans les eaux de surface et souterraines de Guyane. Les*
483 *données des roches totales sont extraites de Gruau et al. (1985); Delor et al. (2001) et Deckart et al. (2005). Les*
484 *données des matières en suspensions de l'Amazonie sont extraites d'Allègre et al. (1996).*
485
486
487

Name	Type	Reference	Well type	lithology
Grand Santi	GWA/alt-sed	MAR201	well in the village (5m)	sand, clays, alluvial deposits
Pompidou	GWA/alt-sed	MAR203	well in the village (5m)	sand, clays, alluvial deposits
Grand Santi	GWA/alt-sed	MAR201	well in the village (5m)	sand, clays, alluvial deposits
Yaou 3	GWA/alt-sed	Y 3	spring from saprolite	meta-volcanic rocks (basalt, amphibolite) Lower Paramaca P
Dorlin14	GWA/alt-sed	D14	spring from saprolite	meta-volcanic rocks (basalt, amphibolite) Lower Paramaca P
Inini	GWA/alt-sed	25	spring	sand, clays, alluvial deposits
Inini	GWA/alt-sed	P8	shallow drill hole (2m)	sand, clays, alluvial deposits
St Eustache	GWA/alt-sed	GUY99-03	spring from saprolite	granitoide, migmatites, Caribbean plutonism ☐
Corossony 1	GWA/alt-sed	GUY99-04	piezometer (10m)	sand, clays developped on granitoides Caribbean plutonism ☐
Corossony 2	GWA/alt-sed	GUY99-05	piezometer (10m)	sand, clays developped on granitoides Caribbean plutonism ☐
Corossony 14	GWA/alt-sed	GUY99-06	piezometer (10m)	sand, clays developped on granitoides Caribbean plutonism ☐
TPS1	GWA/alt-sed	GUY99-07	drill hole (20m)	sand, clays developped on granitoides Caribbean plutonism ☐
Bellevue	GWA/alt-sed	GUY99-08	drill hole (20m)	sand, clays developped on granitoides Caribbean plutonism ☐
MAC1	GWA/alt-sed	GUY99-09	drill hole (20m)	sand, clays developped on granitoides Caribbean plutonism ☐
St Jean	GWA/alt-sed	GUY99-10	well in the village (5m)	sand, clays, alluvial deposits
Javouhey	GWA/alt-sed	GUY99-11	drill hole	sand, clays, littoral deposits
SC8	GWA/alt-sed	GUY99-12	drill hole (20m)	sand, clays, littoral deposits
SC4	GWA/alt-sed	GUY99-13	drill hole (20m)	sand, clays, littoral deposits
Camopi	GWA/bas	CR1	drill hole (30m)	migmatites
Camopi	GWA/bas	CR2	drill hole (20m)	migmatites
Grand Santi	GWA/bas	F1	drill hole (50m)	migmatites
Grand Santi	GWA/bas	F2	drill hole (60m)	migmatites
Grand Santi	GWA/bas	F1/1h	drill hole (50m)	migmatites
Grand Santi	GWA/bas	F1/72h	drill hole (50m)	migmatites
Grand Santi	GWA/bas	F2/72h	drill hole (60m)	migmatites
Grand Santi	GWA/bas	F1	drill hole (50m)	migmatites
Grand Santi	GWA/bas	F2	drill hole (60m)	migmatites
Maripasoula	GWA/bas	M1	drill hole (70m)	meta-volcanic rocks (basalt, amphibolite) Lower Paramaca P
Maripasoula	GWA/bas	M3 bis	drill hole (65m)	meta-volcanic rocks (basalt, amphibolite) Lower Paramaca P
Maripasoula	GWA/bas	M4	drill hole (60m)	meta-volcanic rocks (basalt, amphibolite) Lower Paramaca P
Maripasoula	GWA/bas	M5	drill hole (75m)	meta-volcanic rocks (basalt, amphibolite) Lower Paramaca P
Loka	GWA/bas	L1 bis	drill hole (50m)	meta-volcanic rocks (basalt, amphibolite) Lower Paramaca P
Loka	GWA/bas	L2	drill hole (50m)	meta-volcanic rocks (basalt, amphibolite) Lower Paramaca P
Dorlin	GWA/bas	Ni 5	artesian drill hole (1m ³ /h)	meta-volcanic rocks (basalt, amphibolite) Lower Paramaca P
Marakoutoukoutou	GWA/bas	CRM2	drill hole (90m)	granitoide, Caribbean plutonism
MM4	GWA/bas	GUY99-01	drill hole (100m)	diorites
CAR1	GWA/bas	GUY99-02	drill hole (80m)	Leptyno-amphibolite Ile de Cayenne series
Marakoutoukoutou	GWA/bas	MKT2	drill hole (100m)	granitoide, Caribbean plutonism

Table 1. Groundwater typology, well type and lithology in the extensive sandy-argillaceous terrane from the coastal area and from shallow wells in the alluvia along the Maroni and Oyapock River catchments (GWA/alt-sed) and from deep wells in the basement (GWA/bas).

Table 1. Typologie des eaux souterraines, type d'ouvrage et lithologie dans la zone argillo-sableuse de la zone cotière et des aquifères superficiels des bassins versants du Maroni et de l'Oyapock (GWA/alt-sed) et des ouvrages profonds dans la zone de socle (GWA/bas).

488
489
490
491
492
493
494
495
496
497
498
499
500
501
502
503
504

Name	Type	Reference	EC μS/cm	T °C	pH	Ca	Na	Mg	K	Cl	SO ₄	NO ₃	HCO ₃	Sr	⁸⁷ Sr/ ⁸⁶ Sr	Eps Nd (0)	¹⁴⁷ Sm/ ¹⁴⁴ Nd	Nd ng/l	Sm ng/l	δ ² H	δ ¹⁸ O
															μmol/l						
Grand Santi	GWA/alt-sed	MAR201	39.5	28.5	5.8	85	170	21	13	70	2	10	391	0.321	0.708130	-	-	-	-	-15.7	-3.5
Pompidou	GWA/alt-sed	MAR203	46.4	19.7	5.99	65	249	6	21	160	2	31	200	0.142	0.710147	-	-	-	-	-16.8	-3.3
Grand Santi	GWA/alt-sed	MAR201	46.4	27.8	5	100	152	33	49	149	3	119	300	0.571	-	-	-	-	-	-16.6	-3.4
Yauu 3	GWA/alt-sed	Y 3	58	24.3	6.05	78	109	177	24	67.6	14	dl	505	0.231	0.708453	-	-	-	-	-14.5	-3.3
Dorlin14	GWA/alt-sed	D14	44	23.6	6.94	62	142	116	27	185.9	35	2	205	0.120	0.710646	-	-	-	-	-15.3	-3.3
Inini	GWA/alt-sed	25	40.7	25.6	5.4	10	157	58	10	197	32	6	38	0.033	0.713692	-	-	-	-	-19.2	-3.7
Inini	GWA/alt-sed	P8	21.1	30.7	5.13	5	109	8	13	99	7	3	19	0.021	0.709707	-	-	-	-	-14.3	-2.8
St Eustache	GWA/alt-sed	GUY99-03	39	25.7	4.48	20	175	40	12	185	12	28	-	0.029	0.728571	-12.64	0.1342	123	27.3	-12.4	-3.2
Corossou 1	GWA/alt-sed	GUY99-04	113	33.3	6.19	67	396	86	44	254	9	4	770	0.342	0.709466	-12.00	0.1209	130	26	-10.7	-2.4
Corossou 2	GWA/alt-sed	GUY99-05	67	30.3	5.19	16	2009	49	35	4241	10	dl	210	0.072	0.709461	-10.42	0.1321	65	14.2	-7.9	-2.1
Corossou 14	GWA/alt-sed	GUY99-06	298	29.8	7	228	9468	457	95	10174	70	dl	2680	1.335	0.708714	-11.63	0.1205	134	26.7	-14.4	-3.2
TPS1	GWA/alt-sed	GUY99-07	84	27.7	5.63	34	273	112	58	276	25	dl	410	0.215	0.721651	-13.28	0.1358	297	66.7	-14.7	-3.1
Bellevue	GWA/alt-sed	GUY99-08	27	26.7	4.53	10	123	28	16	106	5	10	150	0.042	0.713712	-11.22	0.1354	39	8.7	-12.6	-3
MAC1	GWA/alt-sed	GUY99-09	23	29.2	4.4	10	95	18	9	51	4	3	70	0.027	0.710370	-17.83	0.1048	96	16.7	-14.1	-3.1
St Jean	GWA/alt-sed	GUY99-10	98	26.2	6.31	235	243	50	104	120	21	dl	740	0.566	0.717093	-	-	-	-	-9.9	-2.5
Javouhey	GWA/alt-sed	GUY99-11	166	28.5	6.56	717	106	46	39	175	3	84	1310	0.284	0.707984	-14.71	0.0858	60	8.6	-11.3	-2.8
SC0	GWA/alt-sed	GUY99-12	281	29.4	6.64	139	1866	290	96	457	14	dl	2160	0.512	0.709211	-10.59	0.1182	752	14.7	-14.4	-3.3
SC4	GWA/alt-sed	GUY99-13	39	29	5.01	23	150	35	23	154	9	dl	110	0.059	0.713266	-9.25	0.1446	62	14.8	-9.7	-2.5
Camopi	GWA/bas	CR1	-	-	-	28	122	33	33	56	5	18	200	0.134	0.723978	-	-	-	-	-12.3	-2.9
Camopi	GWA/bas	CR2	-	-	-	25	109	25	26	59	5	19	150	0.134	0.725469	-	-	-	-	-12.7	-3.1
Grand Santi	GWA/bas	F1	146.9	26.4	6.6	475	365	188	18	45	1	dl	1750	1.027	-	-	0.1172	4	0.9	-16.4	-3.6
Grand Santi	GWA/bas	F2	198.5	26.2	6.93	783	465	208	21	54	7	dl	2200	1.484	-	-	0.1587	8	2.0	-17.8	-3.6
Grand Santi	GWA/bas	F1/1h	181	27.1	6.88	403	426	200	-	59	4	dl	1754	0.913	0.704100	-	-	-	-	-	-
Grand Santi	GWA/bas	F1/72h	148	26.9	6.38	535	478	254	-	62	6	dl	2197	1.142	0.704200	-	-	-	-	-	-
Grand Santi	GWA/bas	F2/72h	196	26.5	6.83	600	474	225	-	70	7	dl	2295	1.142	0.703985	-	-	-	-	-	-
Grand Santi	GWA/bas	F1	176	-	7.16	674	140	189	19	50.7	20	dl	1767	1.244	0.705429	-18.82	0.1512	3	0.7	-	-
Grand Santi	GWA/bas	F2	215	-	6.95	668	445	238	32	84.5	11	2	2231	1.507	0.704584	-	-	-	-	-	-
Maripasoula	GWA/bas	M1	-	-	-	341	581	190	23	84.5	13	dl	1539	1.758	0.703520	-	0.1109	9	1.7	-	-
Maripasoula	GWA/bas	M3 bis	-	-	-	498	410	597	18	59.2	9	dl	2543	2.055	0.704046	-	0.0807	18	2.4	-	-
Maripasoula	GWA/bas	M4	-	-	-	772	476	498	20	56.3	10	2	2979	3.174	0.703624	-	0.0676	8	0.9	-	-
Maripasoula	GWA/bas	M5	-	-	-	317	372	377	28	107.0	6	15	1708	1.689	0.703596	-	0.0850	25	3.5	-	-
Loka	GWA/bas	L1 bis	-	-	-	796	294	288	12	59.2	8	dl	2354	1.975	0.704260	-15.33	0.1257	8	1.6	-	-
Loka	GWA/bas	L2	-	-	-	999	329	310	29	56.3	11	dl	2877	2.192	0.705883	-	0.1076	19	3.3	-	-
Dorlin	GWA/bas	Ni 5	186	24.9	6.22	290	245	415	22	270.4	87	3	1302	2.295	0.704149	-	0.0430	34	2.4	-18.4	-3.7
Marakoutoukoutou	GWA/bas	CRM2	62	-	5.58	88	230	45	19	157	17	64	415	0.459	0.713903	-	-	-	-	-12.7	-3.1
MM4	GWA/bas	GUY99-01	275	26.6	7.18	766	693	312	49	151	32	5	2560	1.507	0.713512	-15.16	0.1348	5	1.1	-17.9	-4
CAR1	GWA/bas	GUY99-02	156	26	6.14	272	471	264	93	149	23	dl	1330	1.666	0.709933	-24.56	0.0890	6	0.8	-15.9	-3.7
Marakoutoukoutou	GWA/bas	MKT2	237	25.6	6.62	518	952	175	82	408	89	2	1885	1.723	0.712861	-	-	-	-	-13.4	-3.2

Table 2. Major field parameters, major and trace elements, and isotopic data (⁸⁷Sr/⁸⁶Sr, δ¹⁸O, δ²H and εNd(0)) in the groundwaters of French Guiana.

Table 2. Paramètres de terrain, éléments majeurs et traces et données isotopiques (⁸⁷Sr/⁸⁶Sr, δ¹⁸O, δ²H et εNd(0)) dans les eaux souterraines de Guyane.